Original Research *Highlight article*

Neural stem cell-derived exosomes facilitate spinal cord functional recovery after injury by promoting angiogenesis

Dong Zhong[1,2], Yong Cao[1,2], Cheng-Jun Li[1,2], Miao Li[1,2], Zi-Jie Rong[1,2], Liyuan Jiang[1,2], Zhu Guo[3], Hong-Bin Lu[2,4] and Jian-Zhong Hu[1,2]

[1]Department of Spine Surgery, Xiangya Hospital, Central South University, Changsha 410008, PR China; [2]Key Laboratory of Organ Injury, Aging and Regenerative Medicine of Hunan Province, Changsha 410008, PR China; [3]Department of Spine Surgery, Affiliated Hospital of Qingdao University, Qingdao, 266003, PR China; [4]Department of Sports Medicine, Research Center of Sports Medicine, Xiangya Hospital, Central South University, Changsha 410008, PR China

Corresponding authors: Jian-Zhong Hu, Email: jianzhonghu@hotmail.com; Hong-Bin Lu, Email: hongbinlu@hotmail.com; Yong Cao, Email: caoyong1912@163.com

Impact statement

The feeble plasticity of SCMECs after trauma is one of the major causes for the exacerbation of SCI. Therefore, improving the regeneration ability of SCMECs is crucial to promote spinal cord functional recovery after injury. Our current study uncovered that NSCs-Exos could promote SCMECs migration, tube formation and proliferation *in vitro*, and further identified that exosomal VEGF-A mediated the pro-angiogenic effect. Furthermore, we observed a remarkable microvascular density increase, spinal cord cavity shrinkage, and motor function recovery in SCI mice treated with NSCs-Exos, which confirmed the therapeutic effects of NSCs-Exos to alleviate SCI. Downregulating VEGF-A partially abolished these effects of NSCs-Exos. This is the first study to reveal that NSCs-Exos has the pro-angiogenic effect on SCMECs by transferring VEGF-A and promote microvascular regeneration and tissue healing, indicating that NSCs-Exos can become a promising therapeutic bioagent for facilitating the functional recovery of SCI.

Abstract

Acute traumatic spinal cord injury is a devastating event without effective therapeutic approach. The feeble plasticity of spinal cord microvascular endothelial cells (SCMECs) after trauma is one of the major causes for the exacerbation of spinal cord injury. Therefore, improving the plasticity and regeneration of SCMECs is crucial to promote recovery after spinal cord injury. For the present study, we explored the influence of exosomes derived from neural stem cells (NSCs-Exos) on the spinal cord microvascular regeneration after spinal cord injury and determined the underlying mechanisms. After the primary NSCs and SCMECs were extracted, exosomes were isolated from NSCs conditioned medium and used to co-incubated with the SCMECs *in vitro*, and then the effect of exosomes on the angiogenic activities of SCMECs was measured. The candidate molecules involved in the NSCs-Exos-mediated angiogenesis were screened using Western blotting. The effect of NSCs-Exos on angiogenesis and spinal cord functional recovery after injury *in vivo* was analyzed. The results demonstrated that NSCs-Exos could enhance the angiogenic activities of SCMECs, and were highly enriched in VEGF-A. The level of VEGF-A was downregulated in NSCs$^{shVEGF\text{-}A}$-Exos and the pro-angiogenic effects on cocultured SCMECs were inhibited. Furthermore, NSCs-Exos significantly accelerated the microvascular regeneration, reduced the spinal cord cavity, and improved the Basso mouse scale scores in spinal cord injury mice. This work provides the evidence of the underlying mechanism of NSCs-Exos-mediated angiogenesis and suggests a novel therapeutic target for spinal cord injury.

Keywords: Spinal cord injury, exosomes, neural stem cell, angiogenesis, VEGF-A

***Experimental Biology and Medicine* 2020; 245: 54–65. DOI: 10.1177/1535370219895491**

Introduction

Acute traumatic spinal cord injury (SCI) is a devastating condition, leading to substantial permanent morbidity.[1] The lack of effective therapeutic approaches for SCI results in heavy burdens on families and societies. Spinal cord microvascular endothelial cells (SCMECs) damage occurs immediately after SCI, and the resulting disrupted local

Copyright © 2020 by the Society for Experimental Biology and Medicine

angiogenesis, reduced blood supply, and interrupted nutrition supply contribute to the poor plasticity of the spinal cord, which is considered to be the key initiator for the secondary injury in SCI.[2,3] Therefore, strategy to facilitate microvascular regeneration in SCI site may provide the necessary scaffolding and nutrition for nerve regeneration and then promote the neurological function recovery.[4,5]

Neural stem cells (NSCs) have a crucial role in the origination and neural tissue repair of cerebral nerve and can differentiate into neuron and neurogliocytes.[6,7] NSCs are recognized as the most promising natural resource for the treatment of nervous system diseases due to their proliferation, renewal, and passage capacities *in vivo* and *in vitro*.[8] A previous study showed that transplantation of NSCs into the mouse SCI model significantly promoted the motor neurological function recovery after injury, indicating that NSCs can modulate the local microenvironment around the injury area.[9] Rosenzwei *et al.*[10] also reported that local transplantation of NSCs could markedly enhance spinal-cord plasticity after SCI in primates.

Recent studies have revealed that stem cells exert the therapeutic role by secreting factors into their surroundings via a paracrine mechanism, e.g. extracellular vesicles. The emerging extracellular vesicles called exosomes, which are 40–150 nm in diameter, have attracted increasing attention in regenerative medicine.[11] Exosomes are important communication medium between cells by carrying different proteins, lipids, RNA (mRNA, noncoding RNA, etc.) and other biological macromolecules, and can affect the physiological function of target cells by regulating the gene expression or protein synthesis.[12,13] Studies also revealed that human adipose mesenchymal stem cells (hADSCs)-derived exosomes injected in and around rodent skin wounds could significantly promote angiogenesis at the lesion site and accelerate wound healing,[14] and direct administration of exogenous stem cell exosomes could facilitate tissue regeneration and repair at the injured site.[15] Rong *et al.*[16] reported that NSC-derived exosomes (NSCs-Exos) attenuated cell apoptosis and neuroinflammation after traumatic SCI by mediating the activation of autophagy. Thus, the present study was designed to investigate whether NSCs-Exos has beneficial effects on SCMECs and in SCI model, and the underlying mechanisms of NSCs-Exos on neurological functional recovery after SCI were also explored.

Materials and methods

Animal ethical statement

All experiment procedures were performed according to the National Institutes of Health guidelines and were approved by the Animal Use and Ethics Committee of Central South University.

Isolation, culture, and identification of SCMECs

Primary SCMECs were extracted from the spinal cord tissue of C57 mice as previously described.[17] SCMECs were purified using CD31 after the emergence of germinal center (Figure 1(A-a)). Briefly, the germinal centers of SCMECs were formed after culture for seven days, the SCMECs were digested using accutase, centrifuged, and co-incubated with CD31 microbeads (Miltenyi Biotec Germany), and then, the cells were passed through an MS/LS sorting column in the magnetic field. After purifying with CD31 microbeads, the cells were cultured with EBM-2 (Lonza, USA). After three days, CD31 (BioLegend USA) expression was evaluated as well as CD144 and CD146 (Abcam UK) expression using

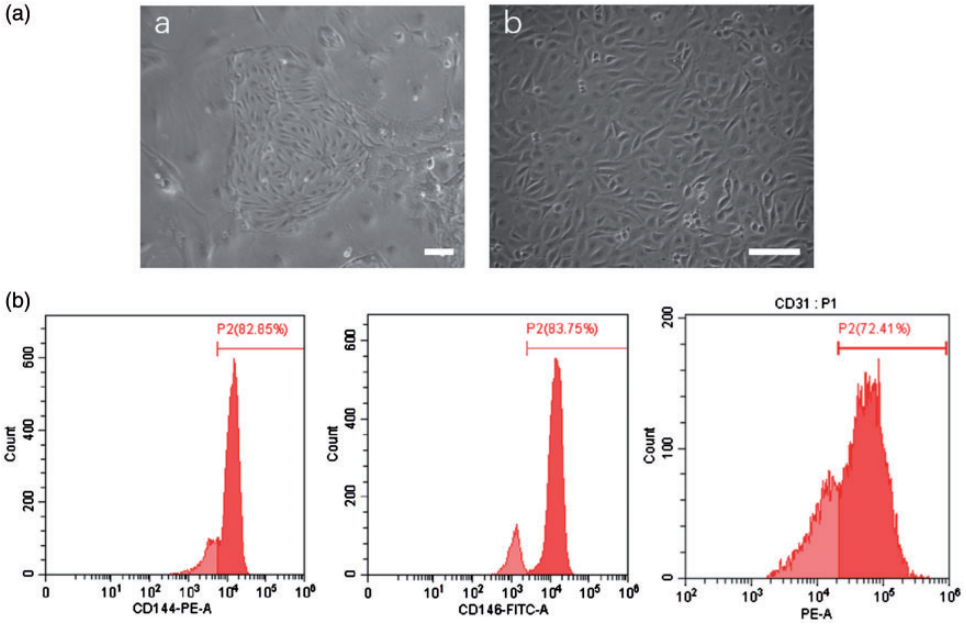

Figure 1. Characterization of mouse primary SCMECs. (a) SCMECs before and after CD31 microbeads purification a: Germinal center of SCMECs before cell purification. Scale bar: 100 μm. b: SCMECs after cell purification. Scale bar: 50 μm. (b) Flow cytometry analysis of the surface markers of SCMECs. The isotype controls are illustrated as light red curves, and the test samples are illustrated as solid dark red curves. (A color version of this figure is available in the online journal.)

flow cytometry instrument (FACS Cant, BD) for identification of SCMECs specificity.

Isolation, culture, and identification of NSCs

A C57 mouse that was pregnant for 14 days was used. NSCs were isolated from cerebral cortex of fetal mouse as previously described.[18] NSCs were cultured in exosome-free mouse NSC culture medium (Cyagen, China) and gently introduced into the cell suspension, passed through a 500-mesh sieve, and inoculated at a density of 1×10^6/mL prior to storage in an incubator. After culturing for seven days, NSCs had a spherical appearance, as shown in Figure 2(a), and neurospheres were centrifuged and plated in a poly-D-lysine-coated coverslip. Multipotent differentiation potentials (including astrocytes, oligodendrocytes and neurons differentiated under different conditions) of NSCs were evaluated by using the different medium. To induce NSC differentiation into astrocytes and oligodendrocyte, NSCs were cultured in DMEM-F12/GlutaMAX^{TM} supplemented with B27 and insulin-like growth factor 1, respectively. Positive GFAP and Olig2 staining confirmed that the NSCs had differentiated into different type of cells, the astrocytes, and oligodendrocytes. When cultured in neural basal medium, NSCs could differentiate into neurons, as confirmed by β-III tubulin immunofluorescent staining. Primary antibodies were listed as follows and diluted as recommended by the specification: Olig2 antibody (ab109186), Nestin antibody (ab6142), GFAP antibody (ab68428), and the β-III tubulin antibody (ab18207), Abcam UK.

Isolation and identification of NSCs-Exos

The supernatant was collected about every three days during NSCs culture, and the dead cells and cell fragments were removed by centrifugation ($300 \times g$ 10 min and $2000g$ 30 min, respectively). After centrifuging the samples ($10{,}000 \times g$ 30 min), the supernatant was filtered by 0.22-μm ultrafiltration and added to the Ultra-15 centrifugal filter (100 kDa; Millipore) and centrifuged at $4000 \times g$ to approximately a 1-mL volume. The ultrafiltration solution was washed with PBS twice, and ultrafiltrated ($4000 \times g$) to approximately 1-mL volume. Then, 1/5 of the volume of

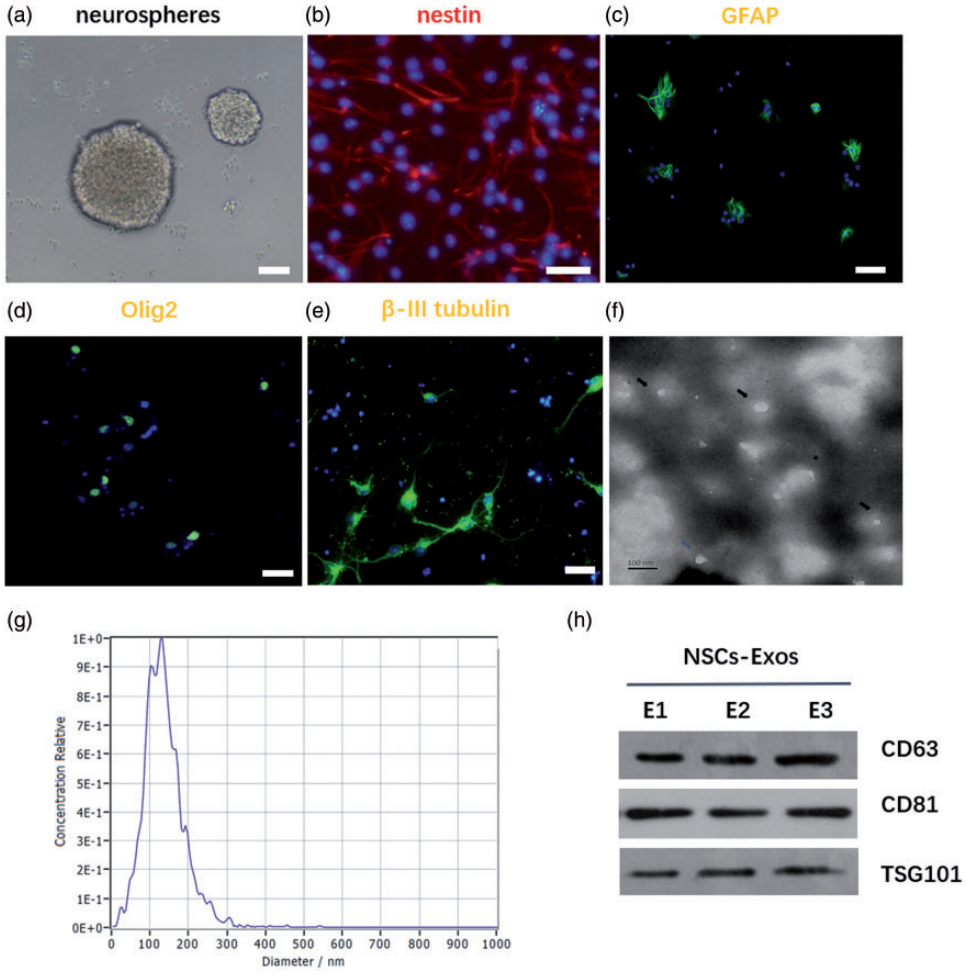

Figure 2. Characterization of NSCs and NSCs-Exos. (a) NSCs showed spherical in shape. Scale bar: 100 μm. (b) Immunofluorescence staining of nestin in NSCs. Scale bar: 100 μm. (c–e) NSCs could differentiate into astrocytes, oligodendrocytes, and neurons under different conditions, as evidenced by GFAP (c), Olig2 (d), and β-III tubulin (e) immunofluorescence staining, respectively. Scale bar: 100 μm. (f) Representative TEM image of exosomes. Scale bar: 100 nm. (g) Size distribution of exosomes based on Malvern Zetasizer Nano ZS90 measurement. (h) Western blot for membrane proteins of NSCs-Exos. (A color version of this figure is available in the online journal.)

exosome external precipitate was added to the superfiltrate. The supernatant was then kept static for 12 h; after the static incubation, the mixture was centrifuged (1500×*g* 30 min) and the supernatant was removed. The isolation exosome was resuspended in 500 μL PBS and was stored in a −80°C refrigerator to be used in additional experiments. Pierce BCA protein assay kit (Thermo Fisher Scientific, USA) was used to test the exosomes protein concentration.

The exosomes suspension was mixed with 4% paraformaldehyde (PFA) and deposited on the EM grid of the formaldehyde coating. A transmission electron microscope (Hitachi h-7650, Tokyo, Japan) was used to test that the exosomes has a typical double-layer membrane structure. Nanoparticle tracking analysis (NTA) further revealed that the mean size of exosomes was 120.6 ± 1.3 nm, and the size was mainly distributed from 40 to 250 nm with a relatively normal distribution. Western blotting verified the expression of a specific marker protein in the exosomes, and as the expression of CD63 and Tsg101 proteins was also observed, monoclonal and antibody diluents were used as follows: CD63 ab217345 Rabbit 1: 1000, UK Abcam; CD81, ab109201 Rabbit 1: 1000, UK Abcam; TSG101, ab125011 Rabbit 1:2000, UK Abcam.

Western blotting analysis

Total protein extraction from NSCs and NSCs-Exos was conducted, and the protein concentrations were detected using Pierce BCA protein kit. Enhanced chemiluminescence reagents (thermoluminescent reagents, Waltham, USA) were used to determine the candidate molecules, including VEGF-A, BDNF, HMGB, Netrin 1, and CTGF, and a chemiluminescence X RS plus luminescence image analyzer (Bio-Rad) was used for imaging. A Gel-pro Analyzer was used to measure the area and gray value of each band, and the gray ratio for each group and the internal reference GAPDH was analyzed to obtain the relative expression level of proteins. Monoclonal antibody diluents were used as follows: VEGF-A, ab52917 Rabbit 1:10,000 UK Abcam; BDNF, ab108319 Rabbit 1:10,000 UK Abcam; HMGB, ab18256 Rabbit 1:1000 UK Abcam; Netrin 1, ab126729 Rabbit 1:10000 UK Abcam; CTGF, ab6992 Rabbit 1:1000 UK Abcam; GAPDH, 10494–1-AP Rabbit 1:3000 Proteintech USA.

qRT-PCR analysis

The total RNA was extracted using TRIzol (Invitrogen, CA, USA), and reverse-transcribed to cDNA using the Prime Script RT Reagent Kit (TaKaRa, Tokyo, Japan). The qRT-PCR was performed using SYBR Premix Ex Taq and specific primers for the target gene. The relative mRNA levels in the target gene were normalized to U6 expression. The expression of target gene among groups was analyzed with the $2^{-\Delta\Delta Ct}$ method. The primer sequences are listed as follows: VEGF-A forward, 5′-CTGTCTAATGCCCTGGAGCC-3′, and reverse, 5′-ACGCGAGTCTGTGTTTTTGC-3′; GAPDH forward, 5′-AGCAAGGACACTGAGCAAGA-3′, and reverse, 5′-GGGGTCTGGGATGGAAATTGT-3′.

VEGF-A deletion using shRNA

A lentivirus short hairpin RNA (shVEGF-A), and the scramble control shRNA (Con shRNA) were generated by Genechem Co. Ltd. (Shanghai, China). The virus packaging was conducted by Genechem. NSCs transfection was conducted according to the manufacturer's instructions. Briefly, the NSCs were incubated in retroviral supernatant. Then, the cells were treated with puromycin (2.5 μg/mL, Sigma) for 72 h after infection. The shRNA sequences are listed as follows: VEGF-A 5′-CCGGCGAGATAGAG TACATCTTCAACTCGAGTTGAAGATGTACTCTATCTC GTTTTTG-3′. Con shRNA: 5′-CCTAAGGTTAAGTCGC CCTCGCTCGAGCGAGGGCGACTTAACCTTAGG-3′.

Exosomes uptake assay

To further explore the characteristics and potential function of NSC-Exos, we used PKH67 (PKH67; Sigma) to label the NSC-Exos as previously described.[19] The SCMECs were incubated with the PKH67-labeled NSC-Exos. After 15 min of incubation, the SCMECs were then fixed with 4% PFA and stained with DAPI (Carlsbad, USA). The uptake of exosome by SCMECs was captured by fluorescence microscopy (Leica DMI6000B, Solms, Germany).

Effects of NSCs-Exos on SCMECs

To detect the effects of NSCs-Exos on the activities of SCMECs, the SCMECs were divided into NSCs-Exos group (100 μg/mL NSCs-Exos), the equivalent amount of PBS control group. n order to detect the role of VEGF-A in NSCs-Exos-mediated activities of SCMECs, SCMECs were cultured in EBM2 (Gibco) with different interventions: PBS, exosomes from Con shRNA-transfected NSCs, $NSCs^{Con\ shRNA}$-Exos, and exosomes from VEGF-A-silenced NSCs $NSCs^{shVEGF\text{-}A}$-Exos.

Proliferation assay. The SCMECs were inoculated into the plate and treated with exosomes. The Cell Counting Kit-8 Reager-8 reagent (Shanghai, China) was added to the medium. After 3 h of incubation, a microplate reader (Bio – 680 Rad, Hercules, USA) was used for the measurement of the absorbance of each well. The average absorbance minus the blank value was used to determine cell proliferation.

Scratch wound healing test. The SCMECs were cultured in 12-wells. After the SCMECs were attached, single membranes were scratched with P-200 tips. Mitomycin-C was added to eliminate the effect of cell proliferation. SCMECs were collected at 0 h, 12 h, and 24 h after scratching. The calculation method of the SCMECs migration area is as previously described.[20]

Transwell migration assay. In this study, we used 24-well transwell to observe SCMECs in their logarithmic growth stage, and a single cell suspension was prepared using medium containing a low concentration of serum (5% FBS). For each well, 1×10^4 cells were used, and three replicates in each group were added to the upper

compartment. Another 500 μL of complete medium was added along with different groups of exosomes (100 μg/mL) or the equivalent amount of PBS. After culturing the cells for 24 h, formaldehyde was used to fix the samples and crystal violet staining was used for observation. Five areas were counted and averaged.

Tube formation analysis. Cold Matrigel (50 μL) was added to 96-well plate, and spread evenly on the bottom; then, the plate was incubated at 37°C incubation to solidify the gel. SCMECs were added to the 96-well plate, and each well contained 2×10^4 cells. Tube formation was observed under a microscope (×100) after 6 h of culture with different treatment.

Construction of mouse SCI model and NSC-Exos treatment

Adult female C57BL/6 mice (25–30 g) were obtained from the Animal Center of Central South University and were housed with free access to food and water. Total 40 experimental mice were randomly divided into the: Sham group (sample size = 10), PBS group (sample size = 10), $NSCs^{shVEGF\text{-}A}$-Exos group (sample size = 10), and $NSCs^{Con\ shRNA}$-Exos group (sample size = 10). Mouse was sacrificed 7 days and 28 days after injury. All the mice in the four groups underwent thoracic vertebral laminectomy of level 10 (T10), and the SCI modeling was conducted using the modified Allen's method to simulate moderate contusion except the Sham Group.[21,22] Briefly, after anesthetizing with pentobarbital sodium (Sigma), a laminectomy at T10 level was performed and subjected to contusive SCI with moderate severity impact (8 g weight × 3 cm vertical height free falling). For different intervention groups, 100 μL PBS, 200 μg $NSCs^{shVEGF\text{-}A}$-Exos in 100 μL PBS, and 200 μg $NSCs^{Con\ shRNA}$-Exos in 100 μL PBS were injected into the tail vein of each mouse, respectively, at 30 min after SCI tills on 3, 6, 9, and 12 post-SCI, respectively.

Lectin staining and microvessel counting

The angiogenesis occurs on day 3 and end ups at 10 days after SCI,[4] so we chose a time point of seven days to observe the vascular recovery. At a given specific time point after observation, the spinal cord vasculature of mice was labeled by tail vein injection of fluorescence-conjugated tomato lectin (Sigma USA), and then the spinal cord, including the T10 level, was harvested to analyze the difference in microvascular density among groups after treatment. Coronal cryostat sections of 15 μm were prepared for microvessel counting using IPP 6.0 (Media Cybernetics). The microvessels counts were calculated as the mean of the number of microvessels obtained from six images.

Behavioral assessment

Locomotion deficits of mice after SCI were measured in an open field according to the BMS Locomotor Rating Scale.[23] The locomotion evaluation was performed before surgery and 1, 3, 7, 14, 21, and 28 days after SCI.

H&E staining and lesion area measurement

At a given specific time point after observation, the spinal cord, including the lesion area at T10, was harvested and prepared for H&E staining to analyze the lesion area among all groups. After deeply anesthetized, mice were transcardially perfused with saline solution and 4% PFA for vessel fixation. The spinal cord was embedded in paraffin, sectioned with 5-μm-thickness in the sagittal plane, and stained with H&E. The section was observed with an Olympus photomicroscope (magnification, ×400). The lesion area was measured using IPP 6.0 (Media Cybernetics).

Statistical analysis

The experimental data were presented as mean ± standard deviation (SD). One-way analysis of variance (ANOVA), followed by the Bonferroni post hoc test was used to assess the significance of differences among different groups. Statistical analysis was performed using GraphPad Prism 7.0 software, and statistically significant differences were considered to be $P < 0.05$.

Results

Characterization of SCMECs

The colonies of SCMECs appeared at three days after the initial separation (Figure 1(a)). Flow cytometry showed that the surface markers of SCMECs, including CD31, CD144, and CD146, were highly positive. CD31-positive cells accounted for 72.41%, CD114-positive cells accounted for 82.85%, and CD146-positive cells accounted for 83.75% of the total cells (Figure 1(b)).

Characterization of NSCs and NSCs-Exos

The NSC neurospheres appeared seven days after the initial separation (Figure 2(a)). Nestin-positive NSCs could differentiate into astrocytes, oligodendrocytes, and neurons under different culture conditions. Astrocytes were large cells with many short protrusions, stellate appearance, abundant cytoplasm, and large nucleus. GFAP-positive cells accounted for 29.8% of the total differentiated cells. The neurons were small and round, with regular shape, smooth edges and spindles, and had 2–3 long protuberance. β-III tubulin-positive cells accounted for 31.8% of the total differentiated cells. Oligodendrocytes were smaller than astroglia, the cell process was short and less, the nucleus was round, small, and dense. Olig2-positive cells accounted for 9.8% of the total differentiated cells. NSCs could differentiate into neurons and glial cells caused by adding into different culture and differentiation conditions (Figure 2(b) to (e)). The vesicles isolated from NSCs conditioned medium were goblet or globular in shape with an average diameter of 120.6 ± 1.3 nm (Figure 2(f) to (g), whose morphology was consistent with those previously reported.[11] Western blot testing identified the exosomal markers, including CD 63 and TSG 101, which further confirmed the exosome identity (Figure 2(h)).

NSCs-Exos promote the angiogenic activities of SCMECs

The NSCs-Exos were transferred to the SCMECs perinuclear region after 12 h co-culture, which indicated that NSCs-Exos could be internalized into the SCMECs and mainly accumulated in the cytoplasm (Figure 3(A-a,b)). The percentage of PKH67-positive cells was $67.8 \pm 8.8\%$ (Figure 3(A-c)).The results of functional experiments showed that the proliferation of SCMECs significantly enhanced under exosome stimulation (Figure 3(b)). NSCs-Exos treatment also promoted the migration of SCMECs, as demonstrated by the scratch trauma test (Figure 3(c) and (d)) and cross-well migration test (Figure 3(e) and (f)). Furthermore, compared with the control group, the SCMECs co-cultured with NSCs-Exos showed a more capillary-like structure. Quantitative analysis showed that

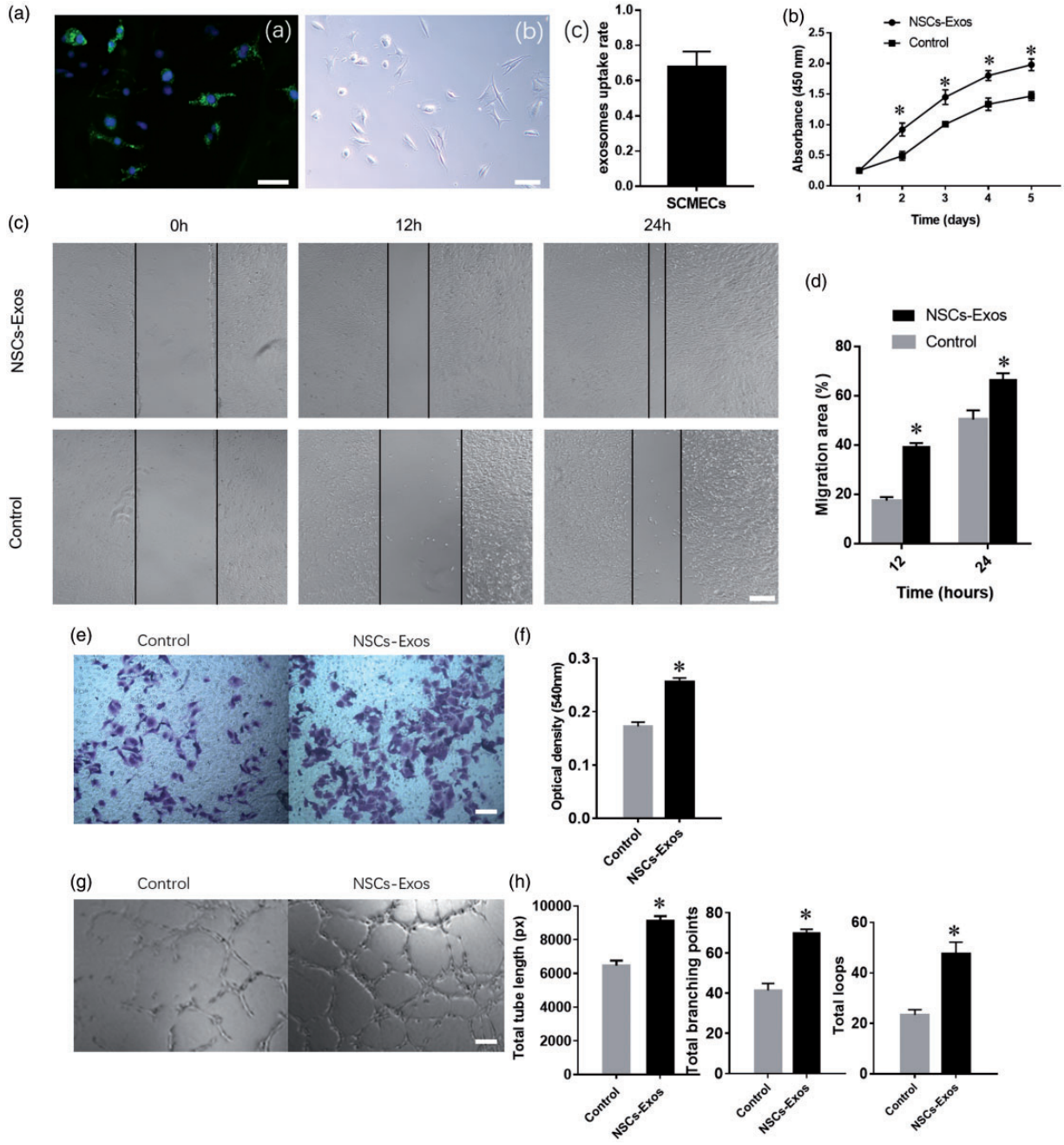

Figure 3. NSCs-Exos promote the angiogenic activities of SCMECs. (A-a) Fluorescence microscopy analysis revealed that PKH67-labeled NSCs-Exos internalization by SCMECs. (A-b) White field image of cells in (A-a) The percentage of PKH67-positive cell (A-c). Scale bar: 50 μm. (b) Proliferation of SCMECs treated with NSCs-Exos or PBS, determined by CCK-8 experiment. $n = 4$ per group. (c) Representative images of scratch wound assay in SCMECs treated with NSCs-Exos or PBS. Scale bar: 250 μm. (d) Quantitative analysis of the migration rate between the two groups at 12 and 24 h in scratch wound assay, $n = 3$ per group. (e) Representative images of migration of SCMECs treated with NSCs-Exos or PBS, detected by transwell assay. Scale bar: 100 μm. (f) Quantitative analysis of the migrated cells between the two groups in transwell assay, $n = 3$ per group. (g) Representative images of tube formation assay on Matrigel in SCMECs treated with NSC-Exos or PBS. Scale bar: 100 μm. (h) Quantitative analyses of the total tube length, total branching points, and total loops in tube formation assay, $n = 3$ per group. *$P < 0.05$, vs. PBS (control) group. (A color version of this figure is available in the online journal.)

the NSCs-Exos group had a remarkable increase in the total branching points, tube length, and loops of SCMECs (Figure 3(g) and (h)). The results revealed that NSCs-Exos could promote the angiogenic activities of SCMECs and may facilitate SCI repair.

Identification of candidate functional molecules in NSCs-Exos

To screen potential functional molecules in NSCs-Exos, we extracted the proteins in NSCs-Exos and determined VEGF-A, BDNF, CTGF, Netrin 1, and HMGB content. Western blot analysis showed that the VEGF-A content in NSCs-Exos was significantly higher compared with other angiogenesis-related proteins (Figure 4(a) and (b)). Furthermore, VEGF-A content in NSCs was significantly lower than that in NSCs-Exos (Figure 4(c) and (d)).

VEGF-A mediates the proangiogenic effect of NSCs-Exos

To further explore the function of VEGF-A in endothelial angiogenesis induced by NSCs-Exos, VEGF-A-silenced shRNA (shVEGF-A) and control shRNA (Con shRNA) were transfected into NSCs, respectively. The VEGF-A expression could be downregulated by shVEGF-A, and Western blot analysis confirmed that VEGF-A level decreased in NSCs$^{shVEGF\text{-}A}$-Exos (Figure 4(e) and (f)). The CCK-8 experiment (Figure 5(a)), scratch wound-healing analysis (Figure 5(b) and (c)), and transwell assay (Figure 5(d) and (e)) demonstrated that the capability of NSCs$^{shVEGF\text{-}A}$-Exos to promote the SCMECs proliferation and migration was attenuated. In contrast to the NSCs$^{Con\ shRNA}$-Exos treatment group, fewer tubular structures were formed on the matrix gel when SCMECs treated with NSCs$^{shVEGF\text{-}A}$-Exos (Figure 5(f)). The downregulation of VEGF-A level in NSCs$^{shVEGF\text{-}A}$-Exos was further confirmed to inhibit the tube formation by quantitative analysis of the total branching points, tube length, and loops of SCMECs (Figure 5(g) to (i)). In general, our results suggested that exosomal VEGF-A was necessary to promote angiogenesis in the spinal cord.

Exosomal VEGF-A accelerates the spinal microvascular regeneration of mice after SCI

The spinal cord microvessel count was determined in four groups (Sham, PBS, NSCsshVEGF-A-Exos, and NSCsCon shRNA-Exos groups) at seven days after SCI, and the results demonstrated that compared to the PBS and NSCs$^{shVEGF\text{-}A}$-Exos treatment groups, the microvascular density of the NSCs $^{Con\ shRNA}$-Exos group was significantly higher (Figure 6(a) and (b)) than that of the PBS and NSCs$^{shVEGF\text{-}A}$-Exos groups.

Exosomal VEGF-A reduces the lesion area and promotes spinal cord functional recovery after injury

H&E staining revealed that the integrity of the spinal cord was destroyed and local cavity formed after SCI, and

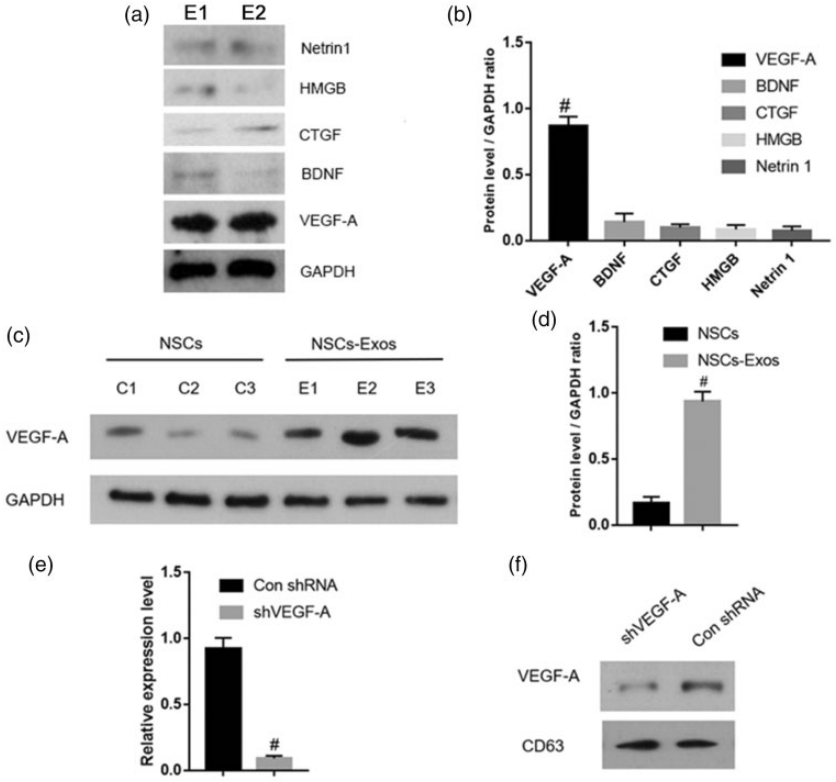

Figure 4. Identification of candidate functional molecules in NSCs-Exos. (a–b) Western blotting and the corresponding quantitative analysis for the angiogenesis-related proteins (including VEGF-A, BDNF, CTGF, HMGB, and Netrin 1) in NSCs-Exos. # $P < 0.05$ vs. other angiogenesis-related proteins. (c–d) Western blotting and the corresponding quantitative analysis for VEGF-A in NSCs or NSCs-Exos. # $P < 0.05$ vs. NSCs. (e) qRT-PCR analysis of VEGF-A expression in NSCs$^{shVEGF\text{-}A}$ or NSCs$^{Con\ shRNA}$, $n = 3$ per group. # $P < 0.05$ vs. NSCs$^{Con\ shRNA}$. (f) Western blot analysis for VEGF-A in NSCs$^{shVEGF\text{-}A}$-Exos or NSCs$^{Con\ shRNA}$-Exos. E1 = exosomes 1, E2 = Exosomes 2. E3 = exosomes; C1 = NSCs1, C2 = NSCs2, C3 = NSCs3.

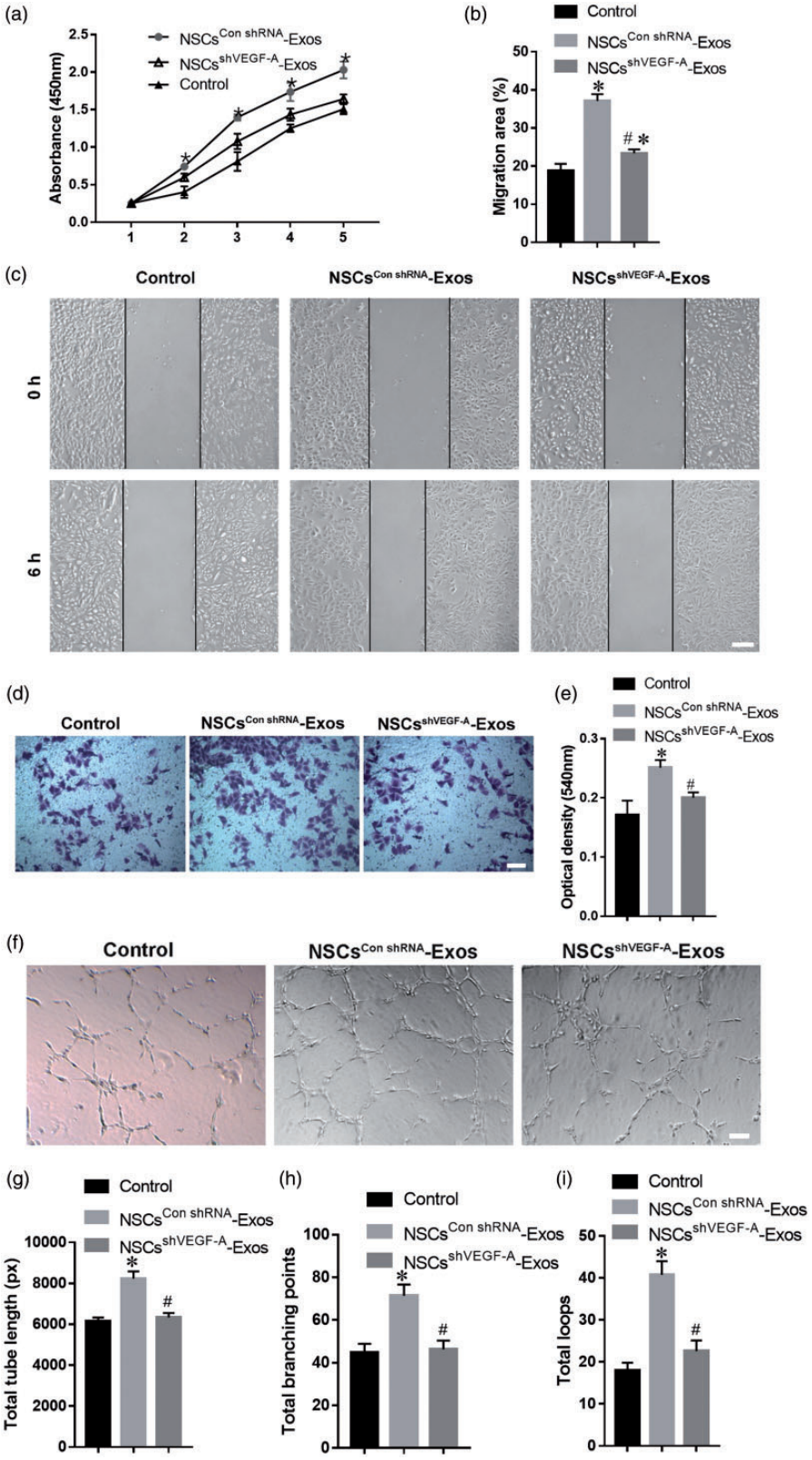

Figure 5. VEGF-A mediates the pro-angiogenic effect of NSCs-Exos. (a) Proliferation of SCMECs treated with PBS (control), NSCs$^{\text{Con shRNA}}$-Exos, and NSCs$^{\text{shVEGF-A}}$-Exos over time, determined by CCK-8 experiment. $n = 4$ per group. (b–e) Representative images and the corresponding quantitative analysis of migration of SCMECs treated with PBS (control), NSCs$^{\text{Con shRNA}}$-Exos, and NSCs$^{\text{shVEGF-A}}$-Exos, assessed by scratch wound assay (b–c) (Scale bar: 250 μm) and transwell assay (d–e) (Scale bar: 100 μm), $n = 3$ per group. (f) Representative images of tube formation assay for SCMECs treated with PBS (control), NSCs$^{\text{Con shRNA}}$-Exos, and NSCs$^{\text{shVEGF-A}}$-Exos. Scale bar: 200 μm. (g–i) Quantitative analyses of the total tube length, total branching points, and total loops in tube formation assay, $n = 3$ per group. *$P < 0.05$, vs. PBS (control) group; # $P < 0.05$ vs. NSCs$^{\text{Con shRNA}}$-Exos group. (A color version of this figure is available in the online journal.)

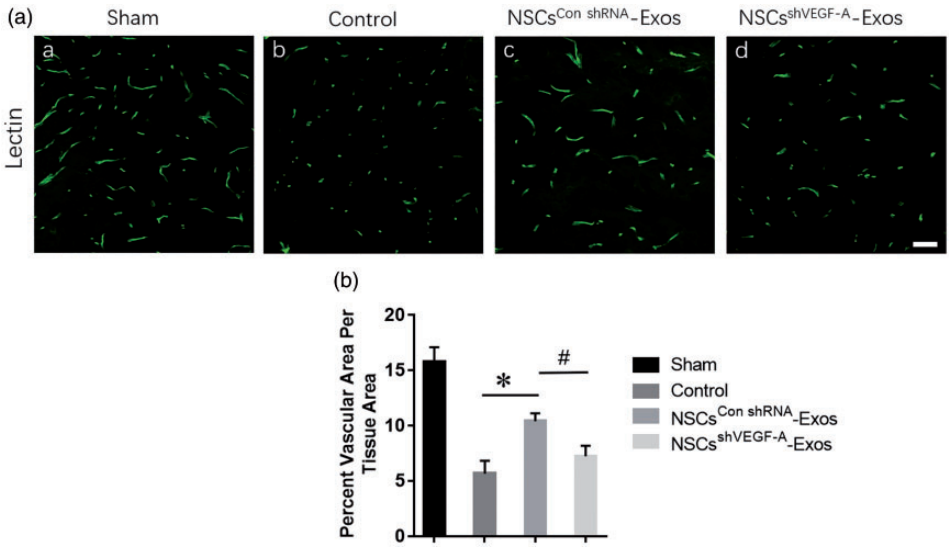

Figure 6. Exosomal VEGF-A accelerates the spinal microvascular regeneration of mice after SCI. (A) Representative photomicrographs for lectin staining of spinal cord microvessels in four different groups: (a) PBS treatment after SCI, (b) only sham operation, (c) NSCs$^{\text{Con shRNA}}$-Exos treatment after SCI, and (d) NSCs$^{\text{shVEGF-A}}$-Exos treatment after SCI. Scale bar = 50 μm. (B) Quantitative analyses of microvessel counts in the four groups. Data are mean ± SD, $n = 5$ per group. *$P < 0.05$, vs. NSCs$^{\text{shVEGF-A}}$-Exos or PBS (control) group; # $P < 0.05$, vs. PBS (control) group. (A color version of this figure is available in the online journal.)

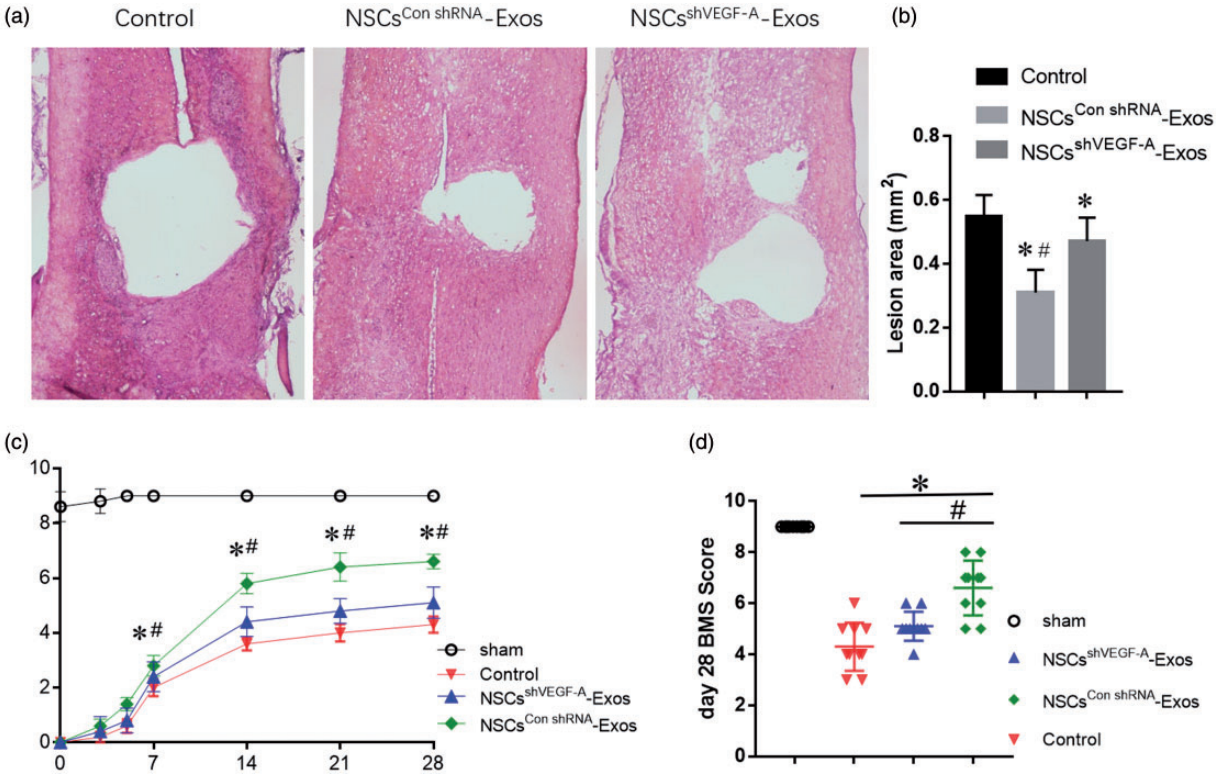

Figure 7. Exosomal VEGF-A shrinks the spinal cord cavity and promotes the functional recovery in mice after SCI. (a–b) Representative HE staining photographs of coronal section of the spinal cord at the injury site 28 days after SCI and the corresponding quantitative analysis of the spinal cord cavity area. (c) The dynamic change of BMS score over time in the NSCs$^{\text{Con shRNA}}$-Exos, NSCs$^{\text{shVEGF-A}}$-Exos, PBS (control), and Sham groups, $n = 10$ per group. (d) The scatter plot of 28th day BMS score in (c). Data are mean ± SD (*$P < 0.01$, vs. PBS (control) group; #$P < 0.01$, vs. NSCs$^{\text{shVEGF-A}}$-Exos group). (A color version of this figure is available in the online journal.)

histopathological changes in the PBS and NSCs$^{\text{shVEGF-A}}$-Exos groups were similar. Nevertheless, the spinal cord cavity in the NSCs$^{\text{Con shRNA}}$-Exos group significantly shrinked compared with the other two SCI groups, as shown by the quantitative analysis of the cavity area (Figure 7(a) and (b)). The functional recovery of mice was observed for three weeks after SCI modeling in four groups to explore whether treatment with NSCs-Exos could rescue the locomotion. BMS score in SCI groups (i.e. PBS, NSCs$^{\text{shVEGF-A}}$-Exos, and NSCs$^{\text{Con shRNA}}$-Exos groups)

rapidly decreased just after contusive SCI. The motor function of hindlimbs improved gradually during the evaluation period in the SCI groups, as demonstrated by increased BMS score. At three days post SCI, the BMS score in the $NSCs^{Con\ shRNA}$-Exos groups (1.40 ± 0.55) showed a better functional recovery than control (0.60 ± 0.55) and $NSCs^{shVEGF\text{-}A}$-Exos groups (0.80 ± 0.45). On the 7th day, the BMS score in the $NSCs^{Con\ shRNA}$-Exos groups (2.80 ± 0.83) is significantly higher than control (2.00 ± 0.70) and $NSCs^{shVEGF\text{-}A}$-Exos groups (2.40 ± 0.55). On the 28th day, the BMS scores for PBS, $NSCs^{shVEGF\text{-}A}$-Exos, and $NSCs^{Con\ shRNA}$-Exos groups were 4.30 ± 0.95, 5.10 ± 0.57, and 6.70 ± 1.25, respectively. As expected, the $NSCs^{Con\ shRNA}$-Exos group showed better BMS scores than the other two SCI groups (Figure 7(c) and (d)). There was no difference in regarding to BMS score between PBS, $NSCs^{shVEGF\text{-}A}$-Exos groups.

Discussion

Our present study revealed that NSCs-Exos could promote SCMECs migration, proliferation, and tube formation *in vitro* and further identified that exosomal VEGF-A mediated the pro-angiogenic effect. Furthermore, we observed a remarkable microvascular density increase, spinal cord cavity shrinkage, and motor function recovery in SCI mice treated with NSCs-Exos, which confirmed the therapeutic effects of NSCs-Exos to alleviate SCI. Downregulating VEGF-A partially abolished these effects of NSCs-Exos. This is the first study to indicate that NSCs-Exos can exhibit pro-angiogenic effect on SCMECs by transferring VEGF-A and promote microvascular regeneration and tissue healing, indicating that NSCs-Exos can become a novel regulator in SCI therapy.

Acute traumatic SCI is a devastating condition, and vascular damage occurs immediately after SCI, which eventually impaired angiogenesis. In this study, we demonstrated that spinal cord microvascular density decreased in SCI mice, which suggested that SCI led to SCMECs angiogenesis dysfunction and was consistent with previous reports.[24] NSCs-based therapy has been taken into account as an ideal candidate for the CNS injury. It has been reported that transplanted NSCs could promote functional recovery in acute SCI[7,25] by differentiating into neurons[26,27] and/or secreting a series of angiogenic factors.[28,29] Nevertheless, the CNS environment around the SCI site is generally not conducive to neuroregeneration.[30] The difficulty of integrating into host tissue, low angiogenic ability, and survival rate of transplanted NSCs influences the outcome of SCI treatment.[25,30] Recently, Ratajczak *et al*.[31] reported that the extracellular vesicles secreted by transplanted NSCs or NSCs-Exos play a vital role in NSCs-mediated paracrine effects. Exosome-based cellular therapy has become an attractive method of tissue engineering due to the following advantages: without risk of immunological rejection, tumorigenicity, and vascular occlusion, high stability, convenience of accessing to wound sites, and decreased potential risks of stem cell therapies.[32,33] Thus, to investigate the effects of NSCs-Exos on SCMECs, we cocultured NSCs-Exos with the SCMECs *in vitro* and found that SCMECs proliferation, migration, and tube formation were significantly enhanced by NSCs-Exos. Our data indicated that NSCs-Exos might improve the angiogenesis abilities of SCMECs, exerting potential therapeutic effects on SCI.

As we know, exosomes can deliver proteins into the target cells through fusing with cellular membranes of recipient cells.[34,35] To determine the functional protein molecules involved in NSCs-Exos-mediated pro-angiogenesis, several angiogenesis-related proteins were measured in NSCs-Exos as well as NSCs. The results showed that VEGF-A content of NSCs-Exos was the highest among the angiogenesis-related proteins, and the VEGF-A was rich in NSCs-Exos rather than NSCs. VEGF-A is an important growth factor in promoting vascular endothelial cells angiogenesis and maintaining vascular integrity.[36] To investigate whether VEGF-A is the key molecular for the observed effects of NSCs-Exos on SCMECs, we tested the role of VEGF-A-knockdown NSCs-Exos in regulating SCMECs angiogenesis. It has been reported that the contents of exosomes could be engineered by modifying the parent cells,[37] and shRNA transfection has been identified as a good tool to modify the exosome contents. In this study, we generated VEGF-A-down expressing NSCs-Exos from shVEGF-A-transfected NSCs. We found that compared with $NSCs^{Con\ shRNA}$-Exos, the level of VEGF-A was downregulated in $NSCs^{shVEGF\text{-}A}$-Exos and the migration, proliferation, and tube formation abilities of cocultured SCMECs were inhibited. This indicated that VEGF-A can be delivered to SCMECs from NSCs by NSCs-Exos, which suggested that NSCs-Exos exerted pro-angiogenic effects on SCMECs probably due to their carried VEGF-A. The role of VEGF-A in promoting vascular endothelial cells angiogenic function is consistent with the previous reports.[38]

Finally, the results from the *in vivo* experiments in SCI mice demonstrated that treatment with NSCs-Exos resulted in the local microvascular density increase, spinal cord cavity shrinkage, and motor function recovery. Meanwhile, the inhibition of VEGF-A in NSCs-Exos led to the suppression of the therapeutic effects, which indicated that exosomal VEGF-A promoted the spinal cord microvascular regeneration and functional recovery after SCI. Acute contusive SCI results in widespread blood vessels damage and consequent local hypoxia within the adjacent to the injury site, which is harmful for nervous tissue regeneration and repair.[39] Thus, NSCs-Exos exerted therapeutic effects in SCI via promoting angiogenesis due to their carried VEGF-A. Notably, the effect of NSCs-Exos on angiogenesis was not completely eliminated by the inhibition of VEGF-A, which suggested that other molecules or signaling pathways may play a role in regulation of microvascular regeneration. The next step in our ongoing research is to conduct proteomics studies to explore the functional proteins involved in pro-angiogenesis and axonal regeneration of NSCs-Exos.

In conclusion, the results demonstrated that NSCs-Exos transferred VEGF-A into SCMECs and promote the angiogenic activities of SCMECs, and treatment with NSCs-Exos could facilitate neurological function recovery after SCI, which largely attributed to the pro-angiogenic effects of

VEGF-A. Therefore, NSCs-Exos with high level of VEGF-A could be potential therapeutic strategy for SCI management and promising area of interest for future clinical trials. However, due to the insufficiency in the investigation on the role and mechanism of exosomal VEGF-A in the angiogenesis and microenvironment of SCI, further experiments are required to further elucidate the intrinsic mechanisms.

Authors' contributions: JZH, HBL and YC designed the experiments. DZ, CJL, ML, ZJR and LYJ conducted the experiments. DZ and YC analyzed the experimented data and prepared all the figures. DZ, XL, CJL, ML, ZJR, and LYJ provided technical support. ZD and ZG wrote the manuscript.

ACKNOWLEDGEMENTS

We would like to thanks Prof. Hui Xie and other staff from the Movement System Injury and Repair Research Center, Xiangya Hospital, Central South University; and Prof. Xianghang Luo and other staff from the Department of Endocrinology, Endocrinology Research Center, Xiangya Hospital of Central South University, for their kind assistance during the experiments.

DECLARATION OF CONFLICTING INTERESTS

The author(s) declared no potential conflicts of interest with respect to the research, authorship, and/or publication of this article.

FUNDING

The author(s) disclosed receipt of the following financial support for the research, authorship, and/or publication of this article: This work was funded by the National Natural Science Foundation of China, NSFC (Nos. 81672174, 81874004, 81902224), and the Natural Science Foundation of Hunan Province (Grant Nos.2019JJ50959) , and the Science Foundation of Xiangya Hospital for Young Scholar (Grant No. 2017Q1).

ORCID ID

Jian-Zhong Hu https://orcid.org/0000-0002-0736-1488

REFERENCES

1. Jain NB, Ayers GD, Peterson EN, Harris MB, Morse L, O'Connor KC, Garshick E. Traumatic spinal cord injury in the United States, 1993-2012. *JAMA* 2015;**313**:2236–43
2. Chen C, Zhang YP, Sun Y, Xiong W, Shields LBE, Shields CB, Jin X, Xu XM. An in vivo duo-color method for imaging vascular dynamics following contusive spinal cord injury. *J Vis Exp* 2017;**130**:e56565
3. Mautes AE, Weinzierl MR, Donovan F, Noble LJ. Vascular events after spinal cord injury: contribution to secondary pathogenesis. *Phys Ther* 2000;**80**:673–87
4. Figley SA, Khosravi R, Legasto JM, Tseng YF, Fehlings MG. Characterization of vascular disruption and blood-spinal cord barrier permeability following traumatic spinal cord injury. *J Neurotrauma* 2014;**31**:541–52
5. Soubeyrand M, Badner A, Vawda R, Chung YS, Fehlings MG. Very high resolution ultrasound imaging for real-time quantitative visualization of vascular disruption after spinal cord injury. *J Neurotrauma* 2014;**31**:1767–75
6. Bond AM, Ming GL, Song H. Adult mammalian neural stem cells and neurogenesis: five decades later. *Cell Stem Cell* 2015;**17**:385–95
7. Martino G, Pluchino S. The therapeutic potential of neural stem cells. *Nat Rev Neurosci* 2006;**7**:395–406
8. Martino G, Pluchino S, Bonfanti L, Schwartz M. Brain regeneration in physiology and pathology: the immune signature driving therapeutic plasticity of neural stem cells. *Physiol Rev* 2011;**91**:1281–304
9. Salazar DL, Uchida N, Hamers FP, Cummings BJ, Anderson AJ. Human neural stem cells differentiate and promote locomotor recovery in an early chronic spinal cord injury NOD-scid mouse model. *PLoS One* 2010;**5**:e12272
10. Rosenzweig ES, Brock JH, Lu P, Kumamaru H, Salegio EA, Kadoya K, Weber JL, Liang JJ, Moseanko R, Hawbecker S, Huie JR, Havton LA, Nout-Lomas YS, Ferguson AR, Beattie MS, Bresnahan JC, Tuszynski MH. Restorative effects of human neural stem cell grafts on the primate spinal cord. *Nat Med* 2018;**24**:484–90
11. Tkach M, Thery C. Communication by extracellular vesicles: where we are and where we need to go. *Cell* 2016;**164**:1226–32
12. Au Yeung CL, Co NN, Tsuruga T, Yeung TL, Kwan SY, Leung CS, Li Y, Lu ES, Kwan K, Wong KK, Schmandt R, Lu KH, Mok SC. Exosomal transfer of stroma-derived miR21 confers paclitaxel resistance in ovarian cancer cells through targeting APAF1. *Nat Commun* 2016;**7**:11150
13. Jiang N, Xiang L, He L, Yang G, Zheng J, Wang C, Zhang Y, Wang S, Zhou Y, Sheu TJ, Wu J, Chen K, Coelho PG, Tovar NM, Kim SH, Chen M, Zhou YH, Mao JJ. Exosomes mediate Epithelium-Mesenchyme crosstalk in organ development. *ACS Nano* 2017;**11**:7736–46
14. Hu L, Wang J, Zhou X, Xiong Z, Zhao J, Yu R, Huang F, Zhang H, Chen L. Exosomes derived from human adipose mensenchymal stem cells accelerates cutaneous wound healing via optimizing the characteristics of fibroblasts. *Sci Rep* 2016;**6**:32993
15. Zhang B, Wu X, Zhang X, Sun Y, Yan Y, Shi H, Zhu Y, Wu L, Pan Z, Zhu W, Qian H, Xu W. Human umbilical cord mesenchymal stem cell exosomes enhance angiogenesis through the Wnt4/beta-catenin pathway. *Stem Cells Transl Med* 2015;**4**:513–22
16. Rong Y, Liu W, Wang J, Fan J, Luo Y, Li L, Kong F, Chen J, Tang P, Cai W. Neural stem cell-derived small extracellular vesicles attenuate apoptosis and neuroinflammation after traumatic spinal cord injury by activating autophagy. *Cell Death Dis* 2019;**10**:340–57
17. Navone SE, Marfia G, Invernici G, Cristini S, Nava S, Balbi S, Sangiorgi S, Ciusani E, Bosutti A, Alessandri G, Slevin M, Parati EA. Isolation and expansion of human and mouse brain microvascular endothelial cells. *Nat Protoc* 2013;**8**:1680–93
18. Ahlenius H, Kokaia Z. Isolation and generation of neurosphere cultures from embryonic and adult mouse brain. *Methods Mol Biol* 2010;**633**:241–52
19. Hu Y, Rao SS, Wang ZX, Cao J, Tan YJ, Luo J, Li HM, Zhang WS, Chen CY, Xie H. Exosomes from human umbilical cord blood accelerate cutaneous wound healing through miR-21-3p-mediated promotion of angiogenesis and fibroblast function. *Theranostics* 2018;**8**:169–84
20. Yu X, Li W, Deng Q, You S, Liu H, Peng S, Liu X, Lu J, Luo X, Yang L, Tang M, Weng X, Yi W, Liu W, Wu S, Ding Z, Feng T, Zhou J, Fan J, Bode AM, Dong Z, Liu J, Cao Y. Neoalbaconol inhibits angiogenesis and tumor growth by suppressing EGFR-mediated VEGF production. *Mol Carcinog* 2017;**56**:1414–26
21. Hu JZ, Huang JH, Zeng L, Wang G, Cao M, Lu HB. Anti-apoptotic effect of microRNA-21 after contusion spinal cord injury in rats. *J Neurotrauma* 2013;**30**:1349–60
22. Cao Y, Wu T, Yuan Z, Li D, Ni S, Hu J, Lu H. Three-dimensional imaging of microvasculature in the rat spinal cord following injury. *Sci Rep* 2015;**5**:12643
23. Basso DM, Fisher LC, Anderson AJ, Jakeman LB, McTigue DM, Popovich PG. Basso mouse scale for locomotion detects differences in recovery after spinal cord injury in five common mouse strains. *J Neurotrauma* 2006;**23**:635–59
24. Cao Y, Zhou Y, Ni S, Wu T, Li P, Liao S, Hu J, Lu H. Three dimensional quantification of microarchitecture and vessel regeneration by synchrotron radiation microcomputed tomography in a rat model of spinal cord injury. *J Neurotrauma* 2017;**34**:1187–99

25. Gincberg G, Arien-Zakay H, Lazarovici P, Lelkes PI. Neural stem cells: therapeutic potential for neurodegenerative diseases. *Br Med Bull* 2012;**104**:7–19
26. Lu P, Wang Y, Graham L, McHale K, Gao M, Wu D, Brock J, Blesch A, Rosenzweig ES, Havton LA, Zheng B, Conner JM, Marsala M, Tuszynski MH. Long-distance growth and connectivity of neural stem cells after severe spinal cord injury. *Cell* 2012;**150**:1264–73
27. Lu P, Woodruff G, Wang Y, Graham L, Hunt M, Wu D, Boehle E, Ahmad R, Poplawski G, Brock J, Goldstein LS, Tuszynski MH. Long-distance axonal growth from human induced pluripotent stem cells after spinal cord injury. *Neuron* 2014;**83**:789–96
28. Jin K, Xie L, Mao X, Greenberg MB, Moore A, Peng B, Greenberg RB, Greenberg DA. Effect of human neural precursor cell transplantation on endogenous neurogenesis after focal cerebral ischemia in the rat. *Brain Res* 2011;**1374**:56–62
29. Jablonska A, Drela K, Wojcik-Stanaszek L, Janowski M, Zalewska T, Lukomska B. Short-Lived human umbilical Cord-Blood-Derived neural stem cells influence the endogenous secretome and increase the number of endogenous neural progenitors in a rat model of lacunar stroke. *Mol Neurobiol* 2016;**53**:6413–25
30. Cusimano M, Biziato D, Brambilla E, Donega M, Alfaro-Cervello C, Snider S, Salani G, Pucci F, Comi G, Garcia-Verdugo JM, De Palma M, Martino G, Pluchino S. Transplanted neural stem/precursor cells instruct phagocytes and reduce secondary tissue damage in the injured spinal cord. *Brain* 2012;**135**:447–60
31. Ratajczak MZ, Jadczyk T, Pedziwiatr D, Wojakowski W. New advances in stem cell research: practical implications for regenerative medicine. *Pol Arch Med Wewn* 2014;**124**:417–26
32. Xin H, Li Y, Chopp M. Exosomes/miRNAs as mediating cell-based therapy of stroke. *Front Cell Neurosci* 2014;**8**:377–87
33. D, Jong OG, V, Balkom BW, Schiffelers RM, Bouten CV, Verhaar MC. Extracellular vesicles: potential roles in regenerative medicine. *Front Immunol* 2014;**5**:608–20
34. Bruno S, Grange C, Deregibus MC, Calogero RA, Saviozzi S, Collino F, Morando L, Busca A, Falda M, Bussolati B, Tetta C, Camussi G. Mesenchymal stem cell-derived microvesicles protect against acute tubular injury. *J Am Soc Nephrol* 2009;**20**:1053–67
35. Bovy N, Blomme B, Freres P, Dederen S, Nivelles O, Lion M, Carnet O, Martial JA, Noel A, Thiry M, Jerusalem G, Josse C, Bours V, Tabruyn SP, Struman I. Endothelial exosomes contribute to the antitumor response during breast cancer neoadjuvant chemotherapy via microRNA transfer. *Oncotarget* 2015;**6**:10253–66
36. de Nigris F, Crudele V, Giovane A, Casamassimi A, Giordano A, Garban HJ, Cacciatore F, Pentimalli F, Marquez-Garban DC, Petrillo A, Cito L, Sommese L, Fiore A, Petrillo M, Siani A, Barbieri A, Arra C, Rengo F, Hayashi T, Al-Omran M, Ignarro LJ, Napoli C. CXCR4/YY1 inhibition impairs VEGF network and angiogenesis during malignancy. *Proc Natl Acad Sci U S A* 2010;**107**:14484–9
37. Li R, Wang Y, Zhang X, Feng M, Ma J, Li J, Yang X, Fang F, Xia Q, Zhang Z, Shang M, Jiang S. Exosome-mediated secretion of LOXL4 promotes hepatocellular carcinoma cell invasion and metastasis. *Mol Cancer* 2019;**18**:18–36
38. Moens S, Goveia J, Stapor PC, Cantelmo AR, Carmeliet P. The multifaceted activity of VEGF in angiogenesis – implications for therapy responses. *Cytokine Growth Factor Rev* 2014;**25**:473–82
39. Oudega M. Molecular and cellular mechanisms underlying the role of blood vessels in spinal cord injury and repair. *Cell Tissue Res* 2012;**349**:269–88

(Received August 30, 2019, Accepted November 26, 2019)